Science and Technology Indonesia
e-ISSN:2580-4391 p-ISSN:2580-4405
Vol. 10, No. 4, October 2025

Research Paper

Wear Characteristics of LAM-Processed Hybrid eSiC-GO Coated Ti-Alloy

Md Abdul Maleque[1*], Rosmia Naping[1], Norshahida Sarifuddin[1], Md Mustafizur Rahman[2], Nurin Wahidah Zulkifli[3]

[1]*Department of Manufacturing and Materials Engineering, Kulliyyah of Engineering, International Islamic University Malaysia, Kuala Lumpur, 50728, Malaysia*
[2]*College of Engineering, Universiti Malaysia Pahang, Pahang, 26300, Malaysia*
[3]*Department of Mechanical Engineering, Faculty of Engineering, University Malaya, Kuala Lumpur, 50603, Malaysia*
***Corresponding author**: maleque@iium.edu.my

Abstract
This study concentrates on the wear characteristics of Ti-alloy coated with environmentally friendly silicon carbide-graphene oxide (eSiC-GO) using the liquid additive manufacturing (LAM) technique. Waste rice husk was utilized to extract eSiC material. The hybrid coating of eSiC-GO on Ti-6Al4V alloy was synthesized via LAM technique. Nine wear test samples were obtained from the Taguchi design of experiments variety of process parameters including current (70 , 80, and 90 A), voltage (20, 25, and 30 V), gas flow rate (15, 20, and 25 L/min), eSiC-GO composition (95-5, 90-10, and 85-15 wt%), and a fixed traverse speed (1 mm/s). An analysis of variance (ANOVA) was performed using design software to ascertain the optimal parameter levels for the LAM technique. Optimal hardness, friction, and wear were achieved in experimental run 8, as evidenced by the experimental results. The findings conclude eSiC-GO coated LAM-processed significantly enhanced friction and wear properties. LAM integrates sustainable materials with additive manufacturing advantages to develop hybrid coatings that augment friction and wear resistance. Consequently, aerospace, automotive, and energy can make tangible and measurable contributions to the United Nations' Sustainable Development Goals.

Keywords
Titanium Alloy, Coatings, Friction-Reducing, Wear-Resistant, Abrasive Wear

Received: 19 April 2025, Accepted: 5 August 2025
https://doi.org/10.26554/sti.2025.10.4.1198-1208

1. INTRODUCTION

Titanium alloys, specifically Ti-6Al4V, are primarily composed of titanium with additions of aluminium and vanadium. These alloys exhibit good mechanical properties, offer higher strength-to-weight ratio, superb corrosion resistance, and biocompatibility (Gupta et al., 2022; Dong et al., 1997; Revankar et al., 2017; Zaniolo et al., 2024). Due to these characteristics feature, titanium-alloys are widely utilized in industries such as aerospace, automotive, energy and medical. However, their poor thermal conductivity, low machinability and poor tribological properties limit their applications (Bodunrin et al., 2021; Veiga et al., 2012; Gupta et al., 2021; Huang et al., 2023). These limitations require ongoing technological advancements to ensure the continued relevance and effectiveness of Ti-alloys in various industrial applications. Moreover, to extend the service life of the components made from Ti-alloys and mitigate the risk of unexpected system failures, surface coatings play a vital role (Zhao et al., 2021; Konovalov et al., 2020; Tüten et al., 2019; Popa et al., 2013).

Single-phase coatings are composed of a single layer or phase of material that is applied on the substrate's surface. The development of single-phase coating from synthetic materials presents substantial potential hazards. In certain applications, environmental concerns arise due to the presence of dangerous chemicals and organic volatile compounds, as well as reliability issues, optimal tribological features, and compatibility challenges (Rosmia et al., 2024). Conversely, hybrid coatings are characterized by the unique characteristics of two or more coating materials, which leads to enhanced functionality and performance in comparison to single-phase coatings (Murari et al., 2023). Maleque et al. (2013) and Yumusak et al. (2022) conducted previous research on the impact of composite coatings on the surface hardness of Ti-alloy. They found that the composite-coated Ti-alloy showed an enhancement of hardness up to three times higher compared to base Ti-alloy. Syaripuddin et al. (2024), examined the hardness and corrosion attributes of deposited layer of diluted nichrome (NiCr) applied to alloy using shielded metal arc welding (SMAW) method. Their findings indicated a significant increase in hardness performance due to the effect of micro-galvanic from the formation of martensitic in weld layer that decreasing the corrosion resistance. Sample NiCr-3 has achieved higher hardness of 742.06 HV. Observation also found that incorporating higher NiCr composition on the weld deposited resulted in

high hardness and decreased corrosion resistance. The performance of Ti-alloys, particularly in tribological and biomedical applications, is expected to be improved through the development of hybrid coatings that incorporate a diverse array of materials, such as ceramics, metals, composites, polymers, and biodegradable polymeric materials (Prakash et al., 2024; Santana et al., 2020). Additionally, the integration of renewable resources materials or recycled waste products towards hybrid coatings is considered as a sustainable approach. The recycling of waste materials for the development of sustainable hybrid coating is emphasized not solely to mitigate environmental issues also to improve the mechanical and wear properties of Ti-alloys.

Liquid additive manufacturing (LAM) is a simple, yet cost-effective approach to the development of hybrid coatings, as it is compatible with a diverse set of hybrid materials. LAM ensures uniform distribution and optimal thickness of the hybrid coating while minimizing waste, thereby providing superior control over the coating process (Jappes et al., 2022). The electrode, melt pool, arc, and adjacent heated areas are effectively shielded from atmospheric contamination by the inert gas shield (argon or helium), thereby reducing oxidation (Gregory, 1978). The LAM technique has been implemented in numerous studies to develop hybrid and single-phase coatings. (Azwan et al., 2019; Bax et al., 2013; Yuan et al., 2022; Sahu et al., 2020; Maleque and Adeleke, 2013). Bello et al. (2020) have previously employed the TIG torch method to create TiC-based composite coatings on the surface of AISI 1040 alloy steel. These coatings incorporate materials such as TiC, TiC/hBN, and TiC/Ni-P-hBN. This research examined the impact of reinforcing ceramic powder mixtures on tribological performance, microstructures, hardness, and surface profiles at high temperatures. The results indicated that the TiC/Ni–P-hBN reinforced composite coating exhibited exceptional tribological and hardness properties at the elevated temperature. In another study, Kumar et al. (2023) utilized the TIG cladding technique to create a hard solid-lubricating clad layer of NiTi, TiO_2, and TiAlN coating on a Ti-6Al-4V substrate. The analysis of hard solid-lubricating clad layer showed defect-free cladding with good metallurgical bonds, two times higher microhardness and better wear resistance compared to the base Ti-alloy material, however, with decrease in the coefficient of friction by14 times. Limited research has been conducted on the utilization of the TIG torch LAM method for hybrid coating on Ti-alloys to improve their tribological properties and hardness.

Comprehensive studies have emphasized the importance of meticulously controlling the process parameters in the TIG torch technique (Chandel et al., 2023; Pavan et al., 2020; Peng, 2012). Parameters include the content and composition, electrode size, argon gas flow rate, travel speed, arc gap length, and current of preplaced powder significantly impact the hardness and tribological performance of the resulting hybrid coating. Thus, mastery of these parameters is crucial for researchers in surface engineering and tribology, as optimizing them is directly related to boost up the functionality and performance of hybrid coatings in industry applications. The study from Rakshith et al. (2022), carried out a parameter optimization to obtain the desired quality characteristics of wear and friction of Ti-6Al4V against alumina (Al_2O_3) on pin-on-disc at room temperature using Taguchi method. It was found that the load has more influence on the wear rate response compared to sliding velocity, but the behaviour was opposite to coefficient of friction. The surface properties of the Ti-6Al4V alloy were enhanced by the development of a high entropy alloy layer from AlCrCoFeMnNi materials using the TIG cladding technique by Alazzawi et al. (2024). Additionally, it assessed the process parameters of TIG clading, including current, scanning speed, and shielding gas flow rate, through the use of the Taguchi method. The cladding layer of Ti-alloy was found to have a dendrite structure formed by FCC + BCC/B2 weave-like BCC/B2 precipitates, with a small amount of Cr/Fe-σ phase in the interdendritic structure. For the Taguchi result, the optimal setting parameters for hardness results were a scanning speed of 0.8 mm/s, a current of 50 A, and an argon flow rate of 12 L/min. However, optimizing process parameters to achieve the best properties via the LAM approach has not been addressed in the literature. Therefore, the current research focuses on the systematically optimizing process parameters to enhance the hardness and wear characteristics of hybrid eSiC-GO coatings developed using LAM technique, wherein the eSiC coating material was synthesized from waste rice husk.

An effective experimental tool is required to identify significant factors for optimization to achieve the desired quality characteristics of the coatings using the LAM technique. The Taguchi design has recently gained recognition for its ability to measure robustness and identify control factors that reduce variability caused by uncontrollable factors or noise. This method involves fewer trials compared to full factorial designs, simplifying the process of optimizing process parameters. Therefore, it was found that the Taguchi approach is very useful for optimizing surface hardness, wear characteristics, and quality, as it provides a systematic and efficient framework (Ye et al., 2023).

It is evident from the previous research that no research has been conducted on the wear characteristics of LAM-processed hybrid eSiC-GO coated Ti-alloy. Moreover, the information on the optimization of process parameters for better coating properties through LAM approach is scarce in literature. Therefore, the goal of this present study is to examine the surface hardness, friction, and wear characteristics of a hybrid eSiC-GO coating that was developed using the LAM technique for tribological applications. This study also aims to optimize process parameters using the Taguchi experimental design of an L9 orthogonal array to investigate their impact on surface hardness, coefficient of friction, and wear rate of hybrid eSiC-GO coated Ti-alloy. Additionally, a wear morphology study on the wear track surface was conducted and presented.

Table 1. Process Parameters and Levels of the Taguchi DOE

Control Parameters	Unit	Level 1	Level 2	Level 3
Composition of eSiC-GO	%	95–5	90–10	85–15
Current	A	70	80	90
Voltage	V	20	25	30
Gas Flow Rate	L/min	15	20	25

Table 2. LAM-Processed Matrix Design

Exp Run	Composition of eSiC-GO (%)	Current (A)	Voltage (V)	Gas Flow Rate (L/min)
1	95-5	70	20	15
2	95-5	80	25	20
3	95-5	90	30	25
4	90-10	70	25	25
5	90-10	80	30	15
6	90-10	90	20	20
7	85-15	70	30	25
8	85-15	80	20	25
9	85-15	90	25	15

2. EXPERIMENTAL SECTION

2.1 Design of Experiment

Taguchi Design of Experiments (DOE) method using an L9 (3^3) orthogonal arrays involving four factors and three levels to optimize the four key process parameters- the composition of eSiC-GO, current, voltage, and gas flow rate.

Minitab statistical software is employed to design the matrix and analyze the impact of these factors on hardness, coefficient of friction, and wear rate. Tables 1 and 2 present the parameters levels and matrix design. This method ensures systematic control for improved coating performance.

2.2 Materials and eSiC-GO Preplacement

The oxidized layer and impurities were removed from the titanium alloy (Ti-6Al4V) substrate (50 × 33 × 10 mm) by abrading it by abrasive paper in running water then subsequently cleansing it using acetone. Its chemical composition is shown in Table 3 (Klimas et al., 2016). A carbo-thermal reduction process was implemented to synthesize eSiC from waste rice husk and carbon black. (acid leaching, mixing and pyrolysis). GO was procured from Innovative Pultrusion Sdn. Bhd.

The furnace was sustained at 1250°C for 3 hours and allowing inert argon gas through the oven to remove gaseous byproducts. A crucible covered with lid contain of eSiC sample was placed to create a controlled environment, enhancing the redox reaction efficiency, as illustrated in Figure 1. The reactions proposed for SiC formation in silica and carbon are presented in Equations (1) to (5):

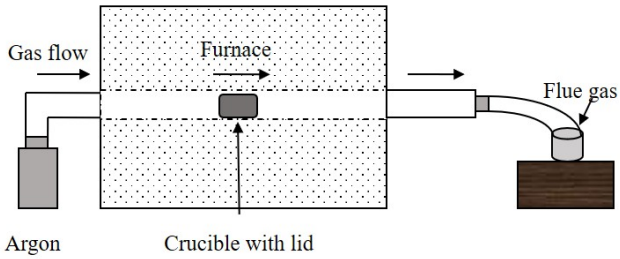

Figure 1. Pyrolysis Process of Synthesizing eSiC (Maleque et al., 2021)

$$SiO_{2(s)} + C_{(s)} = SiO_{(g)} + CO_{(g)} \quad (1)$$

$$SiO_{(g)} + 2C_{(s)} = SiC_{(g)} + CO_{(g)} \quad (2)$$

$$SiO_{2(s)} + 3C_{(s)} = SiC_{(s)} + 2CO_{(g)} \quad (3)$$

$$SiO_{2(s)} + 3C_{(s)} + C_{(s)\,excess} = SiC_{(s)} + 2CO_{(g)} + C_{(s)} \quad (4)$$

$$Si_{(s)} + C_{(s)} = SiC_{(s)} \quad (5)$$

eSiC and GO powders were mixed with DOE ratios, dispersed in distilled water by s ultrasonic bath for 4 hours proceeding to ball milled for 3 hours at 200 rpm (3:1 ball-to-powder ratio). The blended powder was put on Ti-alloy surface at a rate of 0.5 mg/mm^2, dried at 80°C for 1 hour before cooling it down in room temperature.

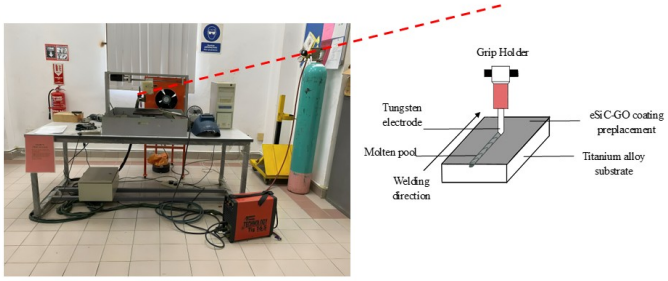

Figure 2. LAM and Experimental Setup Schematic Diagram. (Bello et al., 2020)

Table 3. Chemical Composition of Ti-6Al4V Alloy (Klimas et al., 2016)

Chemical Composition	Al	V	C	Fe	O	N	H	Ti
Weight (%)	6.00	4.00	0.03	0.2	0.15	0.01	0.003	90

2.3 Hybrid eSiC-GO Coating using LAM

The preplacement of eSiC-GO coating was developed through LAM process, which was implemented at a constant speed, 1 mm/s in conjunction to another process variables are outlined in Table 2. The experimental setup for the LAM technique is schematically depicted in Figure 2. Arcs will be produced within the preplaced eSiC-GO surface and the tungsten-thoriated electrode which led to the completely melted formation. and the heat input was calculated using Equation (6) (Gupta et al., 2022). The LAM-processed piece was etched in Kroll's (50% HF, 30% H_2O_2, 20% water) then grounding by abrasive papers, polished using alumina paste after cutting with Wire EDM cutter in natural cooling.

$$\text{Heat Input} = \frac{0.48 \times \text{Current} \times \text{Voltage}}{\text{Electrode Transverse Speed}} \quad (6)$$

2.4 Vickers Hardness Testing

The Wilson Wolpert Vickers hardness tester was employed to conduct Vickers microhardness testing as stated in the ASTM E384 standard. The testing was conducted at a depth of 200 μm, 0.5kgf load and a 10-second delay in indentation. Cross sections hardness samples also measured starting to the middle layer at upper surface down through the substrate material; the collected data then calculated as an average over six measurements.

Table 4. Wear Testing Requirements

Test Standard Parameter	Operating Values
Applied Load, N	30
Frequency, Hz	10
Duration, mins	30
Lubrication Oil	None (Dry condition)
Ball Criterion	
Material	Chromium steel ball
Diameter of the ball, mm	6
Hardness, HRC	62–65

2.5 Tribological Testing

The LAM-processed sample (15×15×6 mm) was polished and cleaned with acetone prior to testing. In dry circumstances, the wear testing with ball-on-disc evaluation was carried out, specified at ASTM D6079 as shown in Table 4. Figure 3 shows the wear test setting up whereas it includes three different views; 3(a) illustrates a wear testing machine photographic view, 3(b) displays the sample arrangement and 3(c) depicts the wear testing schematic diagram. The coefficient of friction data was generated by Winducom Software and from Equation (7), the wear rate was determined.

$$\text{Wear Rate, } W_r = \frac{\Delta m}{L \cdot \rho \cdot F} \quad (7)$$

whereby, Δm is the weight loss (g), L is the sliding distance (m), ρ is the density (g/mm^3), and F is the applied load (N).

3. RESULTS AND DISCUSSION

3.1 Microstructural and Crystaline Structure Analysis

The hybrid coating materials of eSiC and GO were seen in Figure 4. eSiC in Figure 4 (a) showed that the shape has well-arranged micro-bumps. The outer epidermis was discovered to be uneven and to have a highly rigid structure with protrusions with detected carbon particles stick in between silica. From Figure 4 (b), the structured arrangement of carbon atoms forming the hexagonal lattice, portraying the characteristic framework of GO. The tightly woven lattice structure is evident, showcasing the interconnected carbon atoms in their arrangement within the single-layer structure of GO.

Figure 5 shows the plotted XRD of synthesized eSiC after the pyrolysis process. The pattern exhibits a prominent peak of SiO_2 at 2θ = 20.7-23.5° indicating the incomplete reaction or oxidation during the process. The successful formation of SiC was observed at peaks at 2θ = approximately 35°, 41°, 60°, and 72° which confirm the presence of crystalline SiC. The low intensity of SiC peaks represents a partially crystalline or nanocrystalline or amorphous structure. In addition, others silica includes cristobalite of SiO_2 was found at low peak that may formed due to high-temperature reactions during pyrolysis.

3.2 Hybrid Coating Morphology Processed by LAM

The SEM morphology of the hybrid eSiC-GO coated Ti-alloy with varying heat inputs that has been LAM-processed is illustrated in Figure 6. The molten eSiC-GO dispersion exhibited a variety of dendrite morphologies, including tree-like and globular shapes, as a result of the irregular and partially dissolved particles at a higher heat input of 1296 J/mm (Exp. 3). The formation of fine grains was likely impeded by the faster thermal cycles that were associated with the increased heat input, which led to coarser microstructures (Maleque et al., 2018). Experimental runs 5 and 6 exhibited a substantial precipitation of thin dendrites, as did Experimental run 4, which contained 90-10 wt% eSiC-GO. Subsequent analysis confirmed this. In contrast, the microstructure underwent a complete resolidification at a heat input of 768 J/mm (Experimental run 8), which led to a dense population of dendritic precipitates. As detailed in the subsequent section, these dendrites, which encompassed

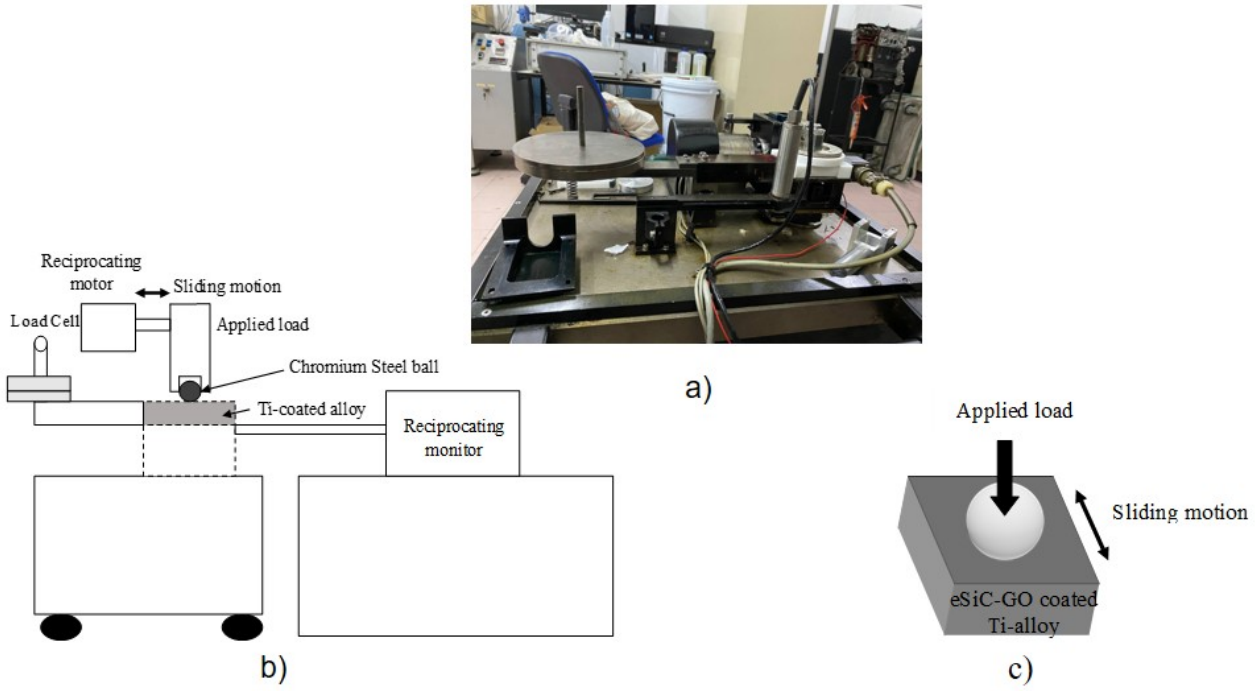

Figure 3. Wear Testing Set-up: (a) Photographic View of the Machine, (b) Sectional View of the Dry Wear Testing and (c) Sample Configuration (Maleque et al., 2021)

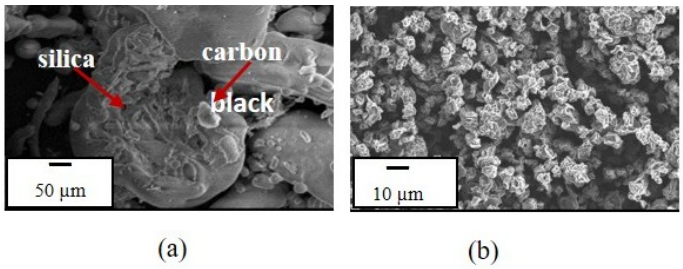

Figure 4. SEM Morphology of (a) eSiC and (b) GO

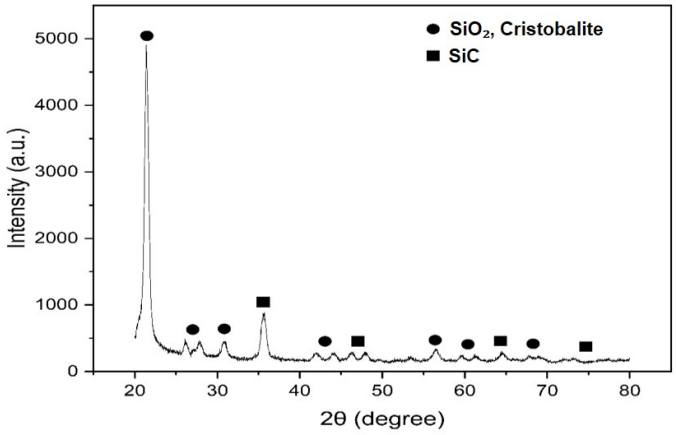

Figure 5. XRD Analysis of Synthesized eSiC

both columnar and equiaxed forms, contributed to the development of hardness on the LAM-processed surface. In general, the microstructures of the LAM-processed hybrid coating on Ti-alloy were comprised of regions with unmelted, partially melted, and fully melted eSiC-GO hybrid coating materials.

3.3 Microhardness

The hardness and signal-to-noise (S/N) ratios of the hybrid eSiC-GO coated material that was LAM-processed are presented in Table 5 for each experimental run. The surface hardness of the hybrid coated material increased by 3-4 times that of the substrate material, as illustrated in Table 5 (324.24 Hv 0.5 kgf). This substantial increase is the result of the complete melting and re-solidification of the hybrid eSiC-GO coating materials with the Ti-alloy, which leads to a more extensive distribution of carbide precipitation. The hybrid eSiC-GO coated Ti-alloy's increase in hardness is a consequence of the LAM method's thorough re-solidification of the melt pool, which has led to the formation of intermetallic compounds and dendritic structures. The friction and wear characteristics of hybrid coated materials can be significantly enhanced due to their increased hardness (Lailatul and Maleque, 2017). The S/N ratio analysis results help to identify the most effective experimental conditions for achieving enhanced hardness in the hybrid eSiC-GO coated Ti-alloy, utilizing the "larger the better" approach as presented by Equation (8) (Gur et al., 2020).

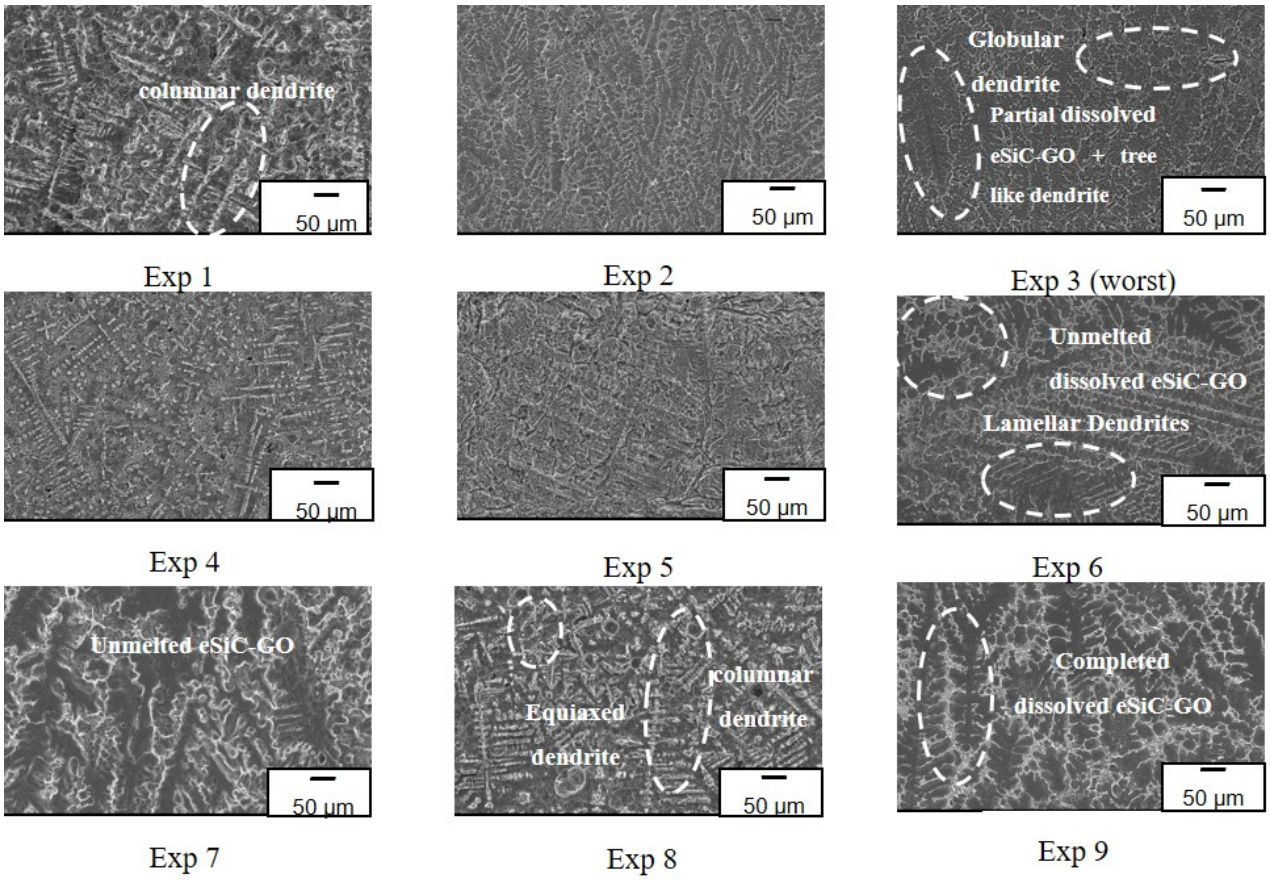

Figure 6. SEM Morphology of LAM-Processed eSiC-GO Coating

Table 5. Vickers Microhardness of the LAM-Processed eSiC-GO Coating According to DOE and Respective S/N Ratio Values

Experimental Run	Vickers Microhardness (Hv)	S/N Ratio (dB)
1	1008.36	60.072
2	1116.98	60.960
3	970.66	59.741
4	1222.37	61.744
5	994.90	59.955
6	1182.21	61.453
7	1203.09	61.606
8	1480.91	63.410
9	1168.79	61.354

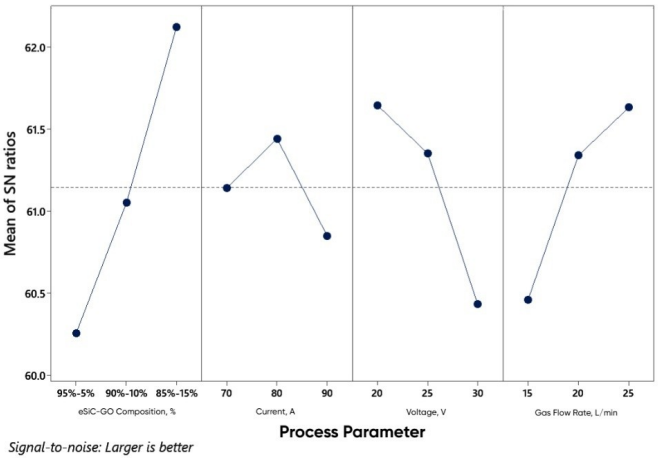

Figure 7. Hardness Main Effects Plot for S/N Ratios in LAM-Processed esic-GO Coating

$$\text{S/N (LTB)} = -10\log_{10}\left(\frac{1}{n}\sum_{i=1}^{n}\frac{1}{y_i^2}\right)\text{ dB} \quad (8)$$

whereby, n is the number of experimental runs in a trial/row, and y_i is the surface hardness value obtained for each respective trial/row.

The eSiC-GO composition parameter is the most influential factor in achieving higher surface hardness, as shown in Table 6, which represents the mean response for the S/N ratio of hardness for the LAM-processed hybrid eSiC-GO coated surface. Other important factors, in order of influence,

Table 6. Hardness Mean Response of S/N Ratio for LAM-Processed eSiC-GO Coating on Ti-Alloy

Level	Composition of eSiC-GO (%)	Current (A)	Voltage (V)	Gas flow rate (L/min)
1	60.26	61.14	61.65	60.46
2	61.05	61.44	61.35	61.34
3	62.12	60.85	60.43	61.63
Delta	1.87	0.59	1.21	1.17
Rank	1	4	2	3

Table 7. CoF Performance of LAM-Processed eSiC-GO Coating According to DOE and Respective S/N Ratio Values

Experimental Run	CoF	S/N ratio (dB)
1	0.19	14.611
2	0.17	15.179
3	0.22	13.348
4	0.12	18.144
5	0.15	16.250
6	0.13	18.009
7	0.10	19.612
8	0.08	21.906
9	0.11	19.243

include voltage, gas flow rate, and current. Figure 7 illustrates the main effects plot for S/N ratios on the hardness of the LAM-processed hybrid eSiC-GO coated surface. The highest points on the graph indicate the optimized process parameters among the others. The optimal parameter settings for surface hardness, in terms of the S/N ratio, are an eSiC-GO composition of 85-15 wt%, a current of 80 A, a voltage of 20 V, and a gas flow rate of 25 L/min.

3.4 Coefficient of Friction (CoF) Analysis

The CoF values are tabulated in Table 7 along with their derived Signal-to-Noise (S/N) ratios. Experiment runs 8 revealed got the lowest CoF, 0.08 compared to Ti-alloy with 0.26 and among other formulations ranging from 0.10 to 0.22. The CoF was reduced by about 70 in comparison to the base Ti-alloy, which caused the creation of an interface thin layer. A solid lubricant of GO resists friction to protect the surface from severe wear in between interacting surfaces (Irawan et al., 2024). The smallest values observed in Experiment runs 8 may contributed in the uniform dispersion of GO material during the surface's sliding and the occurrence of intermetallic elements with a more hardened trait in the LAM-processed eSiC-GO coating Other researchers have conducted an equivalent study into the friction coefficients of titanium alloys contrary to tungsten carbide in dry conditions for sliding (Gur et al., 2020). In evaluating the tribological performance of friction and wear, the data S/N ratios were computed using the "smaller the better" method, as presented by Equation (9),

$$\frac{S}{N}\,(\mathrm{STB}) = -10\log_{10}\left(\frac{1}{n}\sum_{i=1}^{n} y_i^2\right)\ \mathrm{dB} \tag{9}$$

Where by, n is experimental runs number in a trial/row, y_i is the surface CoF and wear rate of each trial/row.

Table 8. CoF mean response of S/N ratio of LAM-processed eSiC-GO coating

Level	Composition of eSiC-GO (%)	Current (A)	Voltage (V)	Gas flow rate (L/min)
1	14.38	17.46	18.18	16.70
2	17.47	17.78	17.52	17.60
3	20.25	16.87	16.40	17.80
Delta	5.87	0.91	1.77	1.10
Rank	1	4	2	3

The ranking of the most influential process parameters is presented in Table 8. From the table, it is evident that the composition of eSiC-GO plays a crucial role as the most significant factor among other process parameters, followed by voltage, gas flow rate, and current, which exert the least effect in improving the friction properties of eSiC-GO hybrid coating on Ti-alloy. Figure 8 illustrates the CoF, main effects plot for S/N ratios of eSiC-GO coated with LAM-processed. The optimal arrangement in accordance with mean S/N ratios values of the LAM process parameters for minimizing friction behavior consists of 85-15 wt% in eSiC-GO composition, 80 A of current, 20 V for voltage, and gas flow rate about 25 L/min.

Table 9. Wear Rate of LAM-Processed eSiC-GO Coating According to DOE and Respective S/N Ratio Values

Experimental Run	Wear Rate ($mm^{-}5/Nm$)	S/N Ratio (dB)
1	2.96	-9.425
2	2.56	-8.164
3	3.52	-10.930
4	1.74	-4.811
5	2.43	-7.712
6	1.98	-5.933
7	1.17	-1.363
8	1.01	-0.086
9	1.49	-3.463

3.5 Wear Rate Analysis

The experimental findings of wear rate, along with the respective S/N ratios for all experimental runs, are presented in Table 9. Once again, Experimental run 8 got lowest wear rate within the nine experiments, exhibiting 1.01 mm^{-5}/Nm, in contrast

Table 10. Wear Rate Mean Response of S/N Ratio in LAM-Processed eSiC-GO Coating

Level	Composition of eSiC–GO (%)	Current (A)	Voltage (V)	Gas flow rate (L/min)
1	-9.507	-5.200	-5.149	-6.867
2	-6.152	-5.321	-5.480	-5.154
3	-1.638	-6.776	-6.669	-5.276
Delta	7.869	1.576	1.520	1.713
Rank	1	3	4	2

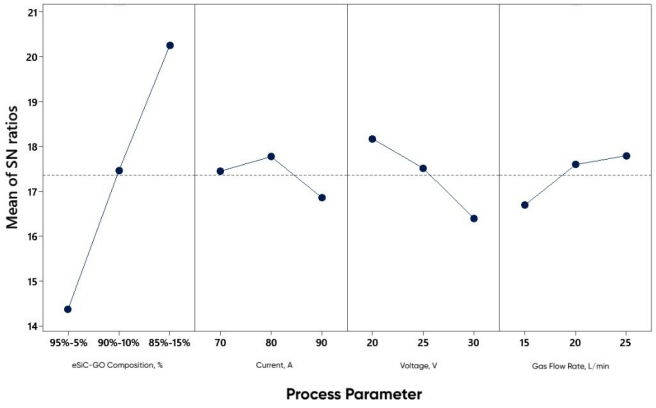

Figure 8. Cof Main Effects Plot for S/N Ratios in LAM-Processed esic-GO Coating

to the substrate Ti-alloy (8.43 mm^{-4}/Nm). This achievement can be attributed to the synergistic effect between the eSiC and GO coating materials, resulting in higher hardness values and lower CoF, thus enhancing the surface characteristics and ultimately leading to the lowest wear rate. Consequently, these coatings appear as the preferred option for applications that necessitate wear-resistant and durable coatings.

Table 10 Illustrates the wear rate mean responses of S/N ratios, highlighting the most impactful factors among the LAM process parameters. The composition of eSiC-GO holds the highest importance as Rank 1, followed by gas flow rate, current, and voltage as Ranks 2, 3, and 4, respectively.

As depicted in Figure 9, the highest points of inclination for each factor denote their significance to the process parameters. Hence, the 85-15 wt% for composition eSiC-GO, 80 A of current, 20 V in voltage, and 20 L/min gas flow rate were identified to be optimum parameters in reducing the impact on the wear rate of the eSiC-GO coated of LAM-processed on Ti-alloy.

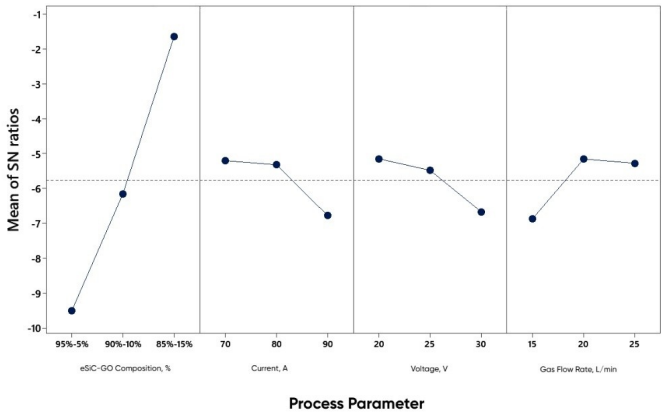

Figure 9. Wear Rate Main Effects Plot for S/N Ratios in LAM-Processed esic-GO Coating

3.6 Wear Morphology Analysis

As illustrated in Figure 10, Experiment 3 displayed the most severe surface damage characterized by adhesive wear. Furthermore, the visibly rougher appearance of the worn surface in Experimental run 3 suggests increased surface-to-surface contact, likely resulting from the higher heat input (such as 1296 J/mm) applied during the LAM process for the development of eSiC-GO hybrid coating on Ti-alloy, indicating signs of thermal degradation or alteration.

Experimental runs of 4, 5, and 6 exhibited similar worn surfaces characterized by striation lines with wear debris and grooves. However, the surface of Experimental run 5 appeared rougher compared to the other experimental runs, particularly due to the 90-10 wt% composition of eSiC-GO.

Conversely, Experimental run 8 exhibited a smooth worn surface with a mild abrasive type of wear, distinguishing it from all other experimental runs. This smoothness can be attributed to the synergetic interaction of the eSiC-GO composition at 85-15 wt% and lower heat input (768 J/mm), which are known to boosted the hardness and improved wear characteristics as mentioned earlier. The wear morphology of the coated surface was also influenced by the composition of GO. A composition of GO led to effects on the worn surface, as GO is known for its excellent properties as a solid lubricant (Taheridoustabad et al., 2021), which minimizes friction between the coated surface and the ball. Graphite thin films layer from carbon-based GO reduce friction and wear by forming a protective, low-shear layer on contact surfaces to reduce metal-to-metal contact.

Superior tribological properties could be achieved based on findings presented. LAM fosters friction- and wear-resistant hybrid coatings using additive manufacturing and sustainable materials. Consequently, industries such as aerospace, automotive, and energy can make tangible and measurable contributions to the United Nations' Sustainable Development Goals. The application of hybrid eSiC-GO coating enhances industrial efficiency with substantially enhancing material dura-

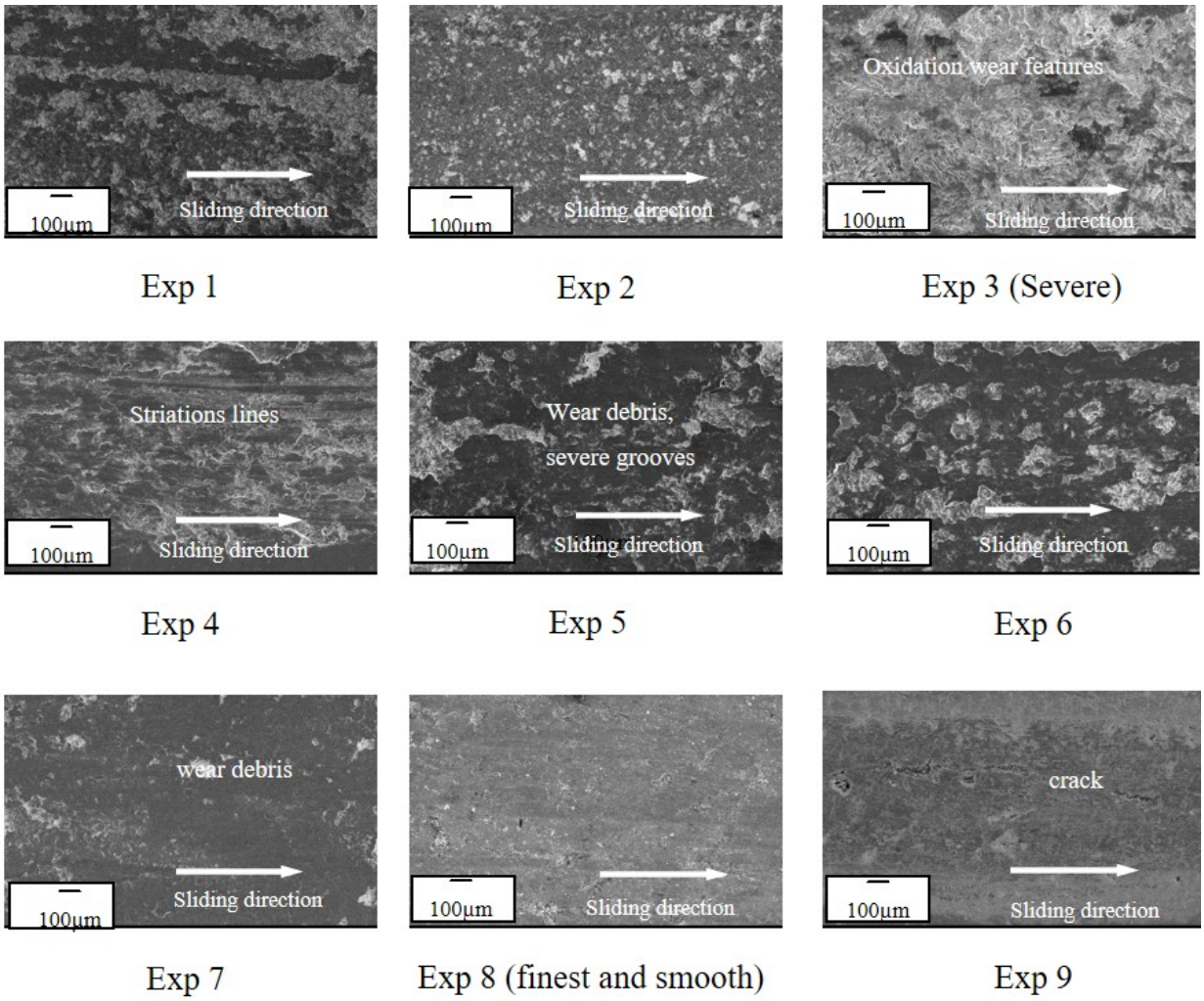

Figure 10. SEM Images of Worn Surfaces of LAM-Processed eSiC-GO Coating on Ti-Alloy

bility and minimizing the maintenance expenses. Moreover, it aligns with the United Nations' Sustainable Development Goals by advocating for sustainable industrial innovation and infrastructure, thereby fostering responsible consumption and production.

4. CONCLUSIONS

In this paper, wear characteristics of LAM-processed eSiC-GO coated Ti-alloy has been presented. Higher hardness properties with 3-4 times more than base Ti-alloy were achieved from intermetallic compounds and dendritic structures formed during the LAM and CoF reduced by 70% owing to high hard surface creating protective films. Experimental runs 8 exhibited lowest wear rate with smooth worn surface and mild abrasive wear resulted to synergetic effect of eSiC-GO materials among other formulations. The optimal parameters for both surface hardness and CoF, in terms of the S/N ratio, are 85-15 wt% for eSiC-GO composition, 80 A in current, voltage about 20 V, and the gas flow rate at 25 L/min. However, eSiC-GO composition plays a crucial role as the most significant factor among other process parameters, followed by voltage, gas flow rate, and current, which exert the least effect in improving the friction properties of hybrid eSiC-GO coated Ti-alloy. To conclude, Experimental runs 8 showed the optimal combination parameters due to its achieved high hardness, lower in coefficient of friction and wear rate making it an ideal for enhanced coating performance. Experimental runs 8 process parameters are closer to the best values demonstrated by Taguchi Method compared to Experiment runs 1. The presented LAM-processed eSiC-GO coating on Ti-alloy exhibited high potential in improved tribological performance. LAM offers to develop the refined of friction and wear sustainable materials of hybrid coatings with benefits of additive manufacturing.

5. ACKNOWLEDGMENT

The project was supported by the Ministry of Higher Education (MOHE) of Malaysia [grant number: FRGS/1/2021/TK0/UIAM/01/1]. The authors would like to express their gratitude

to the International Islamic University of Malaysia (IIUM) for providing technical assistance throughout the study. Additionally, the authors are grateful for the support of Universiti Malaysia Pahang Al-Sultan Abdullah and the University of Malaya (Malaysia).

REFERENCES

Alazzawi, F., H. Aghajani, and A. Kianvash (2024). Surface Improvement of Ti-6Al-4V Alloy by Deposition of AlCrCoFeMnNi High Entropy Alloy Using TIG Process. *JOM*, **76**; 656–666

Azwan, M., M. Maleque, and M. Rahman (2019). TIG Torch Surfacing of Metallic Materials–A Critical Review. *Transactions of the IMF*, **97**; 12–21

Bax, B., M. Schäfer, C. Pauly, and F. Mücklich (2013). Coating and Prototyping of Single-Phase Iron Aluminide by Laser Cladding. *Surface and Coatings Technology*, **235**; 773–777

Bello, K., M. Maleque, and A. Adebisi (2020). Processing of Ceramic Composite Coating via TIG Torch Welding Technique. In S. Hashmi and I. A. Choudhury, editors, *Encyclopedia of Renewable and Sustainable Materials*, volume 4. Elsevier, pages 523–535

Bodunrin, M., L. Chown, and J. Omotoyinbo (2021). Development of Low-Cost Titanium Alloys: A Chronicle of Challenges and Opportunities. *Materials Today: Proceedings*, **38**; 564–569

Chandel, D., L. Thakur, and V. Kumar (2023). An Investigation on the Tribological Behaviour of AlCrCuNiFe High Entropy Alloy Optimized TIG Weld Cladding in Room Temperature Conditions. *Tribology International*, **189**; 108982

Dong, H., A. Bloyce, P. Morton, and T. Bell (1997). Surface Engineering to Improve Tribological Performance of Ti–6Al–4V. *Surface Engineering*, **13**; 402–406

Gregory, E. (1978). Hardfacing. *Tribology International*, **11**; 129–134

Gupta, M., H. Etri, M. Korkmaz, N. Ross, G. Krolczyk, J. Gawlik, N. Yasar, and D. Pimenov (2022). Tribological and Surface Morphological Characteristics of Titanium Alloys: A Review. *Archives of Civil and Mechanical Engineering*, **22**; 72

Gupta, M., Q. Song, Z. Liu, M. Sarikaya, M. Mia, M. Jamil, A. Singla, A. Bansal, D. Pimenov, and M. Kuntoglu (2021). Tribological Performance-Based Machinability Investigations in Cryogenic Cooling Assisted Turning of α-β Titanium Alloy. *Tribology International*, **160**; 107032

Gur, A., C. Ozay, and B. Icen (2020). Evaluation of B4C/Ti Coating Layer, Investigation of Abrasive Wear Behaviors Using Taguchi Technique and Response Surface Methodology. *Surface Review and Letters*, **27**; 1950225

Huang, J., W. Zhang, W. Fang, and Y. Yi (2023). Tribology Properties of Additively Manufactured Ti6Al4V Alloy After Heat Treatment. *Tribology International*, **185**; 108485

Irawan, D., H. D. Saktiioto, W. Bambang, and Sutoyo (2024). High Sensitivity *CH4* and *CO2* Gas Sensor Using Fiber Bragg Grating Coated with Single Layer Graphene. *Science and Technology Indonesia*, **9**(3); 710–717

Jappes, J., A. Ajithram, M. Adamkhan, and D. Reena (2022). Welding on Ni Based Super Alloys–A Review. *Materials Today: Proceedings*, **60**; 1656–1659

Klimas, J., A. Łukaszewicz, M. Szota, and K. Laskowski (2016). Work on the Modification of the Structure and Properties of Ti6Al4V Titanium Alloy for Biomedical Applications. *Archives of Materials Science and Engineering*, **78**; 10–16

Konovalov, S., K. Osintsev, A. Golubeva, V. Smelov, Y. Ivanov, X. Chen, and I. Komissarova (2020). Surface Modification of Ti-Based Alloy by Selective Laser Melting of Ni-Based Superalloy Powder. *Journal of Materials Research and Technology*, **9**; 8796–8807

Kumar, M., S. Kumar, K. Jha, and A. Mandal (2023). Deposition of Hard Solid-Lubricating Composite Coating on Ti-6Al-4V Alloy with Enhanced Mechanical, Corrosion, and Electrical Discharge Wear Properties. *Surface and Coatings Technology*, **457**; 129315

Lailatul, P. and M. Maleque (2017). Surface Modification of Duplex Stainless Steel with SiC Preplacement Using TIG Torch Cladding. *Procedia Engineering*, **184**; 737–742

Maleque, M. and S. Adeleke (2013). Surface Alloying of CP-Ti Using Preplaced Fe-C-Si Powder by Tungsten Inert Gas Torch Technique. In *International Conference on Mechanical, Industrial and Materials Engineering*. pages 668–673

Maleque, M., K. Bello, M. Idriss, and S. Mirdha (2013). Processing of TiC-CNT Hybrid Composite Coating on Low Alloy Steel Using TIG Torch Technique. *Applied Mechanics and Materials*, **378**; 259–264

Maleque, M., L. Harina, and K. Bello (2018). Tribological Properties of Surface Modified Ti-6Al-4V Alloy Under Lubricated Condition Using Taguchi Approach. *Jurnal Tribologi*, **17**; 15–28

Maleque, M., H. Masjuki, K. Low, and M. Ali (2021). Sustainable eSiC Reinforced Composite Materials – Synthetization and Characterization. In *AIP Conference Proceedings of Brunei International Conference on Engineering and Technology 21 (BICET2021), UTB, Brunei*, volume 2643. AIP Publishing, pages 1–6

Murari, G., B. Nahak, and T. Pratap (2023). Hybrid Surface Modification for Improved Tribological Performance of IC Engine Components–A Review. *Proceedings of the Institution of Mechanical Engineers, Part E: Journal of Process Mechanical Engineering*; 09544089221150718

Pavan, A., B. Arivazhagan, and M. Vasudevan (2020). Process Parameter Optimization of A-TIG Welding on P22 Steel. In *Structural Integrity Assessment: Proceedings of ICONS 2018*. Springer, pages 99–113

Peng, D. (2012). Optimization of Welding Parameters on Wear Performance of Cladded Layer with TiC Ceramic via a Taguchi Approach. *Tribology Transactions*, **55**; 122–129

Popa, M., C. Vasilescu, S. Drob, P. Osiceanu, M. Anastasescu, and J. Calderon-Moreno (2013). Characterization and Corrosion Resistance of Anodic Electrodeposited Titanium Oxide/Phosphate Films on Ti-20Nb-10Zr-5Ta Bioalloy. *Journal of the Brazilian Chemical Society*, **24**; 1123–1134

Prakash, P., S. Barnwal, P. Shukla, J. Mehta, P. Kumar, and R. Tewari (2024). Gelatin-Based Forsterite–Hydroxyapatite Hybrid Coating on Ti6Al4V to Improve Its Biocompatibility and Corrosion Resistance. *International Journal of Materials Research*, **115**; 39–46

Rakshith, B., S. Chandraker, and D. Kumar (2022). Optimization of Tribological Parameters to Enhance Wear and Friction Properties of Ti6Al4V Alloy Using Taguchi Method. *Proceedings of the Institution of Mechanical Engineers, Part J: Journal of Engineering Tribology*, **236**; 9

Revankar, G., R. Shetty, S. Rao, and V. Gaitonde (2017). Wear Resistance Enhancement of Titanium Alloy (Ti–6Al–4V) by Ball Burnishing Process. *Journal of Materials Research and Technology*, **6**; 13–32

Rosmia, N., M. Maleque, N. Sarifuddin, M. Hassan, and K. Bello (2024). Contemporary Progress in the Hybrid Coating of Titanium Alloys Using the Liquid Additive Manufacturing Technique. *Journal of Advanced Research in Applied Mechanics*, **113**; 108–117

Sahu, A., A. Raheem, M. Masanta, and C. Sahoo (2020). On the Constancy in Wear Characteristic of Large Area TiC–Ni Coating Developed by Overlapping of TIG Arc Scanning. *Tribology International*, **151**; 106501

Santana, J., S. Kunst, C. Oliveira, A. Bastos, M. Ferreira, and V. Sarmento (2020). PMMA-SiO_2 Organic-Inorganic Hybrid Coating Application to Ti-6Al-4V Alloy Prepared Through the Sol-Gel Method. *Journal of the Brazilian Chemical Society*, **31**; 409–420

Syaripuddin, S., M. Putra, M. Ajiriyanto, S. Yudanto, M. Hasbi, and F. Susetyo (2024). Nichrome Dependency in Welding Layer Using In Situ Fabrication on Hardness and Corrosion Properties. *Science and Technology Indonesia*, **9**(3); 651–659

Taheridoustabad, I., M. Khosravi, and Y. Yaghoubinezhad (2021). Fabrication of GO/RGO/TiC/TiB2 Nanocomposite Coating on Ti–6Al–4V alloy using Electrical Discharge Coating and Exploring its Tribological Properties. *Tribology International*, **156**; 106860

Tüten, N., D. Canadinc, A. Motallebzadeh, and B. Bal (2019). Microstructure and Tribological Properties of TiTaHfNbZr High Entropy Alloy Coatings Deposited on Ti6Al4V Substrates. *Intermetallics*, **105**; 99–106

Veiga, C., J. Davim, and A. Loureiro (2012). Properties and Applications of Titanium Alloys: A Brief Review. *Reviews on Advanced Materials Science*, **32**; 133–148

Ye, Q., Y. Yan, X. Zhang, X. Chen, W. Bai, S. Liu, and F. Zhou (2023). Mechanochemical In-Situ Construction of Ionic Liquid-Functionalized Covalent Organic Frameworks for Anti-Wear and Friction Reduction. *Tribology International*, **189**; 109027

Yuan, W., J. Xu, L. Yu, L. Ge, and Y. Cheng (2022). Effect of Y-Modified TiB_2 Ceramic Particles on the Microstructure and Mechanical Properties of TIG Welded Joints of Spray-Formed 7055 Aluminum Alloy. *Journal of Materials Research and Technology*, **20**; 3126–3135

Yumusak, G., A. Leyland, and A. Matthews (2022). A Microabrasion Wear Study of Nitrided α-Ti and β-TiNb PVD Metallic Thin Films, Pre-Deposited onto Titanium Alloy Substrates. *Surface and Coatings Technology*, **442**; 128423

Zaniolo, K., M. Biaggio, S. Cirelli, M. Cominotte, N. Bocchi, R. Rocha-Filho, and C. Souza (2024). Production and Characterization of Bioactive and Antimicrobial Titanium Oxide Surfaces with Silver Nanoparticles and a Poly (Lactic Acid) Microfiber Coating. *Journal of the Brazilian Chemical Society*, **35**; 1–14

Zhao, Y., Z. Fan, Q. Tan, Y. Yin, M. Lu, and H. Huang (2021). Interfacial and Tribological Properties of Laser Deposited TiOxNy/Ti Composite Coating on Ti Alloy. *Tribology International*, **155**; 106758

